

# Electrochemical Performance of LiFePO<sub>4</sub>/C via Coaxial and Uniaxial Electrospinning Method

Yan Hu, Dawei Gu, Hongying Jiang, Lei Wang, Hongshun Sun, Jipeng Wang, Linjiang Shen\*

College of Sciences, Nanjing Tech University, Nanjing, China

Email: hutengyan512@163.com, dwgu@njtech.edu.cn, jhy@njtech.edu.cn, wang1055@njtech.edu.cn, njutshs@126.com, wjp@njtech.edu.cn, ljshen@njtech.edu.cn

Received 22 March 2016; accepted 16 April 2016; published 19 April 2016

Copyright © 2016 by authors and Scientific Research Publishing Inc.

This work is licensed under the Creative Commons Attribution International License (CC BY).

<http://creativecommons.org/licenses/by/4.0/>



Open Access

---

## Abstract

In this work, LiFePO<sub>4</sub>/C (LFP/C) cathode materials with superior electrochemical performance have been prepared by coaxial and uniaxial electrospinning method. The electrode materials were characterized by X-ray diffraction (XRD), scanning electron microscopy (SEM), and transmission electron microscopy (TEM). Also, cyclic voltammetry (CV), galvanostatic charge-discharge, and electrochemical impedance spectroscopy (EIS) measurements were performed on these materials. The experimental results indicate that the electrochemical properties of LFP/C-C, such as specific capacity, coulombic efficiency, Li<sup>+</sup> diffusion coefficient and overpotential are significantly improved. The enhanced electrical conductivity and polarization of the LFP/C-C electrode are mainly due to its porous morphology and amorphous carbon coating layer.

## Keywords

LiFePO<sub>4</sub>/C, Electrospinning, Porous Structure, Diffusion Coefficient

---

## 1. Introduction

Increased production and usage of electric vehicles and hybrid vehicles in recent years have accelerated the development of the lithium-ion battery (LIB) [1]. As one of the most promising cathode materials in lithium ion batteries, olivine-structured LiFePO<sub>4</sub> (LFP) has attracted significant attention since the initial groundbreaking work was conducted in 1997 by Goodenough *et al.* [2]. LFP exhibits several advantageous features for energy storage, such as high theoretical capacity (170 mAhg<sup>-1</sup>), acceptable operating voltage (3.4 V vs. Li<sup>+</sup>/Li), low cost, environmental friendliness and excellent intrinsic stability [3] [4]. Unfortunately, LFP has several draw-

\*Corresponding author.

backs, including poor electrical conductivity (about  $10^{-9}$  -  $10^{-10}$  S·cm<sup>-1</sup>) [5] and a relatively low Li<sup>+</sup> diffusion coefficient ( $\sim 10^{-14}$  cm<sup>2</sup>·s<sup>-1</sup>) [6] [7], which limit its applications. Several research efforts have focused on developing techniques to overcome these drawbacks, and some of the successful approaches include carbon coating [8] [9], metal ion doping [10] [11], and reduction of LFP particle size [12]-[14]. Moreover, using porous active LFP materials can also help to improve the basic technical parameters of LIBs. The porous active materials typically show excellent electrochemical performance due to their significantly higher specific surface area, which helps the charge transfer between electrode and electrolyte, as well as more available paths for the permeation of ions. The porous electrode materials can be prepared by many different ways, such as catalytic chemical vapor deposition (CCVD) [15], hydrothermal method [16] [17], sol-gel method [18], microwave irradiation assisted synthesis (MIAS) [19] [20], solvothermal method [21] [22], self-assembly [23], and carbothermal reduction method [24].

The electrospinning technique has been widely employed to fabricate various functional materials. In particular, the electrode materials of LiFePO<sub>4</sub> are usually obtained by sintering an electrospun precursor. The electrochemical performance of the electrode material can be greatly enhanced by using this preparation method. For example, single-crystalline nanowires of LiFePO<sub>4</sub>/C with excellent electrochemical performance have been prepared by uniaxial electrospinning [25]. These nanowires grow along the c-axis with uniform distribution of the carbon layer. The carbon layer forms an effective conductive carbon network and shortens the diffusion path along the b-axis, resulting in good cycling capability and rate performance. Tiaxial nanowire of LiFePO<sub>4</sub>/C with core-shell structure have also been prepared using this technique [26], and their unique structure not only helps increased electron conduction path, but also effectively inhibits the oxidation of Fe<sup>2+</sup>.

In this paper, porous nanofibers of LiFePO<sub>4</sub>/C were successfully prepared by sintering the fibers obtained via coaxial electrospinning method. For comparison purposes, LiFePO<sub>4</sub>/C nanofibers were also prepared by the uniaxial electrospinning method. The physical, chemical and electrochemical properties of both nanofibers were measured and characterized, and some meaningful results were acquired. The properties of LiFePO<sub>4</sub> prepared by coaxial electrospinning are obviously better than those by uniaxial electrospinning.

## 2. Experimental

### 2.1. Synthesis

The LiFePO<sub>4</sub>/C nanofibers were prepared by the coaxial electrospinning method. The three starting materials, LiH<sub>2</sub>PO<sub>4</sub> (0.02 M), Fe(NO<sub>3</sub>)<sub>3</sub>·9H<sub>2</sub>O (0.02 M), and 1.0 g of polyoxyethylene (PEO), were ultrasonically dissolved into 40 ml water to form the core solution for spinning. Then, 0.6 g of PEO was ultrasonically dissolved into 40 ml water to obtain the shell solution. These core and shell solutions were filled into different syringes connected to coaxial needles. A direct current electric field of 23 kV was applied between the needle and the target used for collection. A flow rate of 0.9 ml·h<sup>-1</sup> was used in the spinning process. Finally, the as-spun fibers were separated from the target, and then sintered under Ar gas flow (7%: H<sub>2</sub>) as per the following conditions: 1) calcined at 400°C for 5 h; and 2) sintered at 750°C for 12 h, successively. The as-prepared LiFePO<sub>4</sub>/C is denoted by LFP/C-C. Furthermore, an aqueous solution of LiH<sub>2</sub>PO<sub>4</sub> (0.02 M), Fe(NO<sub>3</sub>)<sub>3</sub>·9H<sub>2</sub>O (0.02 M), and 1.0 g of polyoxyethylene (PEO) was prepared as described above. The mixed solution of LiH<sub>2</sub>PO<sub>4</sub>/PEO/Fe(NO<sub>3</sub>)<sub>3</sub>·9H<sub>2</sub>O was filled into the syringe to form uniaxial fibers of precursor. Using the same preparation procedure as for LFP/C-C, uniaxial fibers of the LiFePO<sub>4</sub>/C active material were obtained and denoted as LFP/C-U.

### 2.2. Characterization of the Materials

The crystal structures of the final products were analyzed by X-ray diffraction (XRD), using a DX-2000 X-ray diffractometer (Dandong Haoyuan Instrument Co. Ltd., China) with Cu-K $\alpha$  radiation ( $\lambda = 1.5406$  Å). The sample morphologies were observed by scanning electron microscopy (SEM, JSM-5900, Japan). Transmission electron microscopy (TEM) images were obtained using a transmission electron microscope (JEM 2100F, Japan) with an acceleration voltage of 200 kV. The electrical conductivity of the samples was measured by a four-probe test platform (SB 120/2, China). Surface area of the samples was measured using a specific surface area and pore size analyzer (ST-2000, Qing Tiankang Electronic Technology Co. Ltd., China).

### 2.3. Electrochemical Measurements

Electrochemical characterization of the samples was performed using CR2025 coin-type cells assembled in an

Ar-filled glove box (ZKX-1, Nanjing nine Automation Technology Co. Ltd., China). About 80 wt% of the active material (LFP/C-C or LFP/C-U) was mixed with 10 wt% acetylene black and 10 wt% polyvinylidene in a suitable amount of N-methylpyrrolidone solvent to form slurry. The cathode electrode of the cell was prepared by coating the slurry onto an Al foil. The test cell consisted of the cathode and Li-foil anode separated by a microporous polypropylene membrane (Celgard 2400, Celgard, Inc., USA). The electrolyte was 1 M  $\text{LiPF}_6$  in a solvent mixture of ethylene carbonate (EC) and dimethyl carbonate (DMC) (1:1, v/v). The galvanostatic charge-discharge investigation was carried out on a battery measurement system (Land CT2001A, Wuhan Jinnuo Electricals Co. Ltd., China) within a voltage range of 2.5 - 4.4 V at room temperature. The cyclic voltammetry (CV) and electrochemical impedance spectroscopy (EIS) measurements were performed with an electrochemical workstation (Zahner, Zahner-Elektrik GmbH Co. KG., Germany).

### 3. Results and Discussion

The LFP/C-C and LFP/C-U samples were characterized by XRD (**Figure 1**). The XRD patterns of both materials are similar and match well with the standard pattern (JCPDS card no. 40 - 1499). It is clear that the main diffraction peaks are narrow and strong, showing high crystallinity of the samples. Since both LFP/C-C and LFP/C-U samples were prepared in argon atmosphere, it is believed that residual carbon exists in the samples. However, no diffraction peaks of carbon can be observed in the XRD patterns of LFP/C-C and LFP/C-U in **Figure 1**, even though the theoretical carbon content is about 15 wt% for these samples. Therefore, it can be reasonably assumed that the residual carbon is in amorphous form in the samples.

SEM micrographs of LFP/C-U and LFP/C-C as well as those of their precursors are shown in **Figure 2**. The micrograph of the precursor of LFP/C-U (**Figure 2(b)**) clearly shows that the surface of sample is smooth and the diameters of the fibers are in the range between 200 and 400 nm. From the micrograph of LFP/C-U (**Figure 2(a)**), it can be seen that the sample surface is still very smooth. An obvious difference between **Figure 2(b)** and **Figure 2(a)** is that the size of the former is three times larger than that of the latter. For the sample of LFP/C-C, the micrograph of its precursor shows that the fibers are mostly broken (**Figure 2(d)**). It must be noted that a porous morphology is observed for LFP/C-C (**Figure 2(c)**). As is well known, porous structure of the electrode material is beneficial to the redox reaction. The direct effect of porous structure is greatly increased contact area between the active material and electrolyte. The specific surface areas of both LFP/C-U and LFP/C-C were measured using a specific surface area and pore size analyzer. The specific surface area of LFP/C-U is 30.9841  $\text{m}^2/\text{g}$ , while that of LFP/C-C is as high as 45.5988  $\text{m}^2/\text{g}$ . Hence, it can be expected that the electrochemical performance of LFP/C-C would be better than that of LFP/C-U.

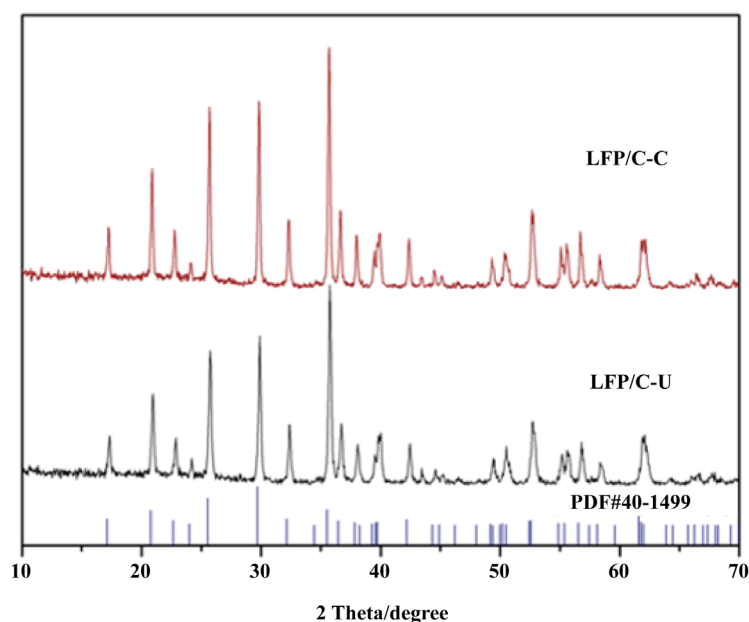


**Figure 1.** XRD patterns of LFP/C-C and LFP/C-U.

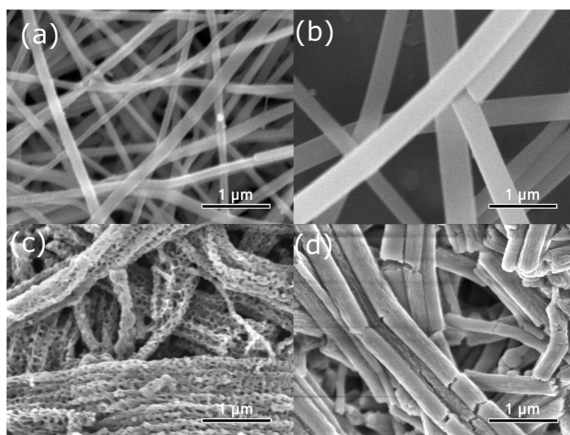


**Figure 2.** SEM images of LFP/C-U (a) and corresponding precursor (b). SEM images of LFP/C-C (c) and corresponding precursor (d).

TEM micrographs of LFP/C-U and LFP/C-C, including HRTEM images, are shown in **Figure 3**. The amorphous layer of carbon in both LFP/C-U and LFP/C-C can be observed in the HRTEM images (**Figure 3(b)** and **Figure 3(d)**). The thickness of the amorphous layer is 3 nm for LFP/C-U, and 4 nm for LFP/C-C. The amorphous carbon layer appears to be coated on the surface of the fibers. This can effectively improve the electrical conductivity of electrode materials. Indeed, the measurements of conductivity confirm that the electrical transport properties of LFP/C-U and LFP/C-C are significantly improved. Using a standard four probes measurement technique, the conductivity values of LFP/C-U (0.81 S/cm) and LFP/C-C (1.20 S/cm) were measured and found to be much higher than those reported by other references. For example, the values of conductivity for LFP/C with fiber morphology previously reported are  $1.9 \times 10^{-4}$  S/cm [27] and  $9.8 \times 10^{-2}$  S/cm [28]. Therefore, the results of conductivity measurements also support the fact that the fibers of LFP in LFP/C-U and LFP/C-C are coated by the amorphous carbon layer.

In order to study the intrinsic kinetics of the lithium ion in LFP/C-C and LFP/C-U, cyclic voltammetry (CV) experiments were carefully performed over a range of scanning rates from 0.1 to 1  $\text{mV}\cdot\text{s}^{-1}$ . One pair of redox peaks can be observed in the CV curves measured at various scanning rates for LFP/C-U (**Figure 4(a)**) and LFP/C-C (**Figure 4(b)**). The redox peaks correspond to the transformation of  $\text{Fe}^{2+}/\text{Fe}^{3+}$  phases, indicating that the lithium ion extraction/insertion reactions in the active material are reversible. The overpotential ( $\Delta V$ ) between the oxidation and reduction peaks derived from the CV curves increases gradually as the scan rate ( $v$ ) increases, suggesting that the electrode material becomes more polarized with increasing scan rates. The  $\Delta V$  values determined in this work for LFP/C-C and LFP/C-U are lower than those reported by other research groups. For example, the  $\Delta V$  values from the CV curves measured at 0.1  $\text{mV}\cdot\text{s}^{-1}$  are 0.24 V (LFP/C-C) and 0.31 V (LFP/C-U), which are significantly lower than the results measured at similar conditions previously reported by Kim *et al.* [29] ( $\Delta V = 0.90$  V) and Lalia *et al.* [30] ( $\Delta V = 0.42$  V). Obviously, the polarization of LFP/C is related to the preparation method of the samples. Moreover, it is expected that the LFP/C prepared through electrospinning will have enhanced electrochemical properties, such as coulomb efficiency.

Diffusion coefficient of the lithium ion is an important factor in the electrochemical performance of a lithium ion battery. The relationships between peak currents ( $I_p$ ) and square root of scan rate ( $v^{1/2}$ ) for LFP/C-U and LFP/C-C are shown in **Figure 4(c)** and **Figure 4(d)**, respectively. The diffusion coefficient of Li ions ( $D$ ) in the electrode can be determined using the Randles-Sevcik equation [19] [31], as follows:

$$I_p = 2.69 \times 10^5 A C D^{1/2} n^{3/2} v^{1/2} \quad (1)$$

where  $I_p$  is the peak current,  $A = 0.785 \text{ cm}^2$  is the effective area of the electrode,  $C = 0.0228 \text{ mol}\cdot\text{cm}^{-3}$  is the bulk concentration of  $\text{Li}^+$  in the electrode,  $D$  is the diffusion coefficient of  $\text{Li}^+$ ,  $n$  is the number of electrons involved in the redox process (for  $\text{Fe}^{2+}/\text{Fe}^{3+}$ ,  $n = 1$ ), and  $v$  is the potential scan rate. The values of  $\text{Li}^+$  diffusion coefficient for LFP/C-U and LFP/C-C are listed in **Table 1**. As mentioned earlier, the LFP/C sample prepared by sintering the coaxial precursor, *i.e.* LFP/C-C, consists of porous nanofibers. Such a porous structure provides a considerably large contact area between the electrode materials and the electrolyte, which facilitates deeper penetration of

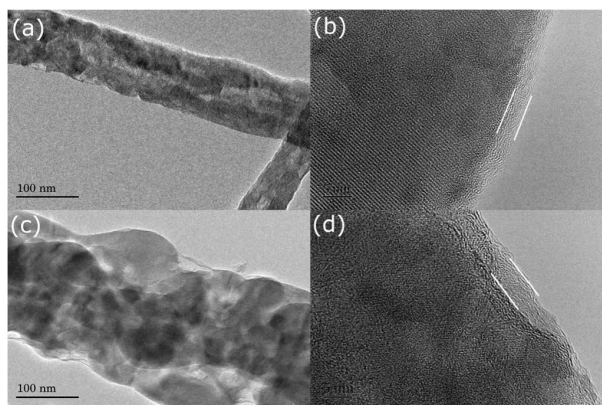


**Figure 3.** TEM micrograph of LFP/C-U and the corresponding HRTEM image are shown in (a) and (b), respectively. TEM micrograph of LFP/C-C and HRTEM image are shown in (c) and (d), respectively.

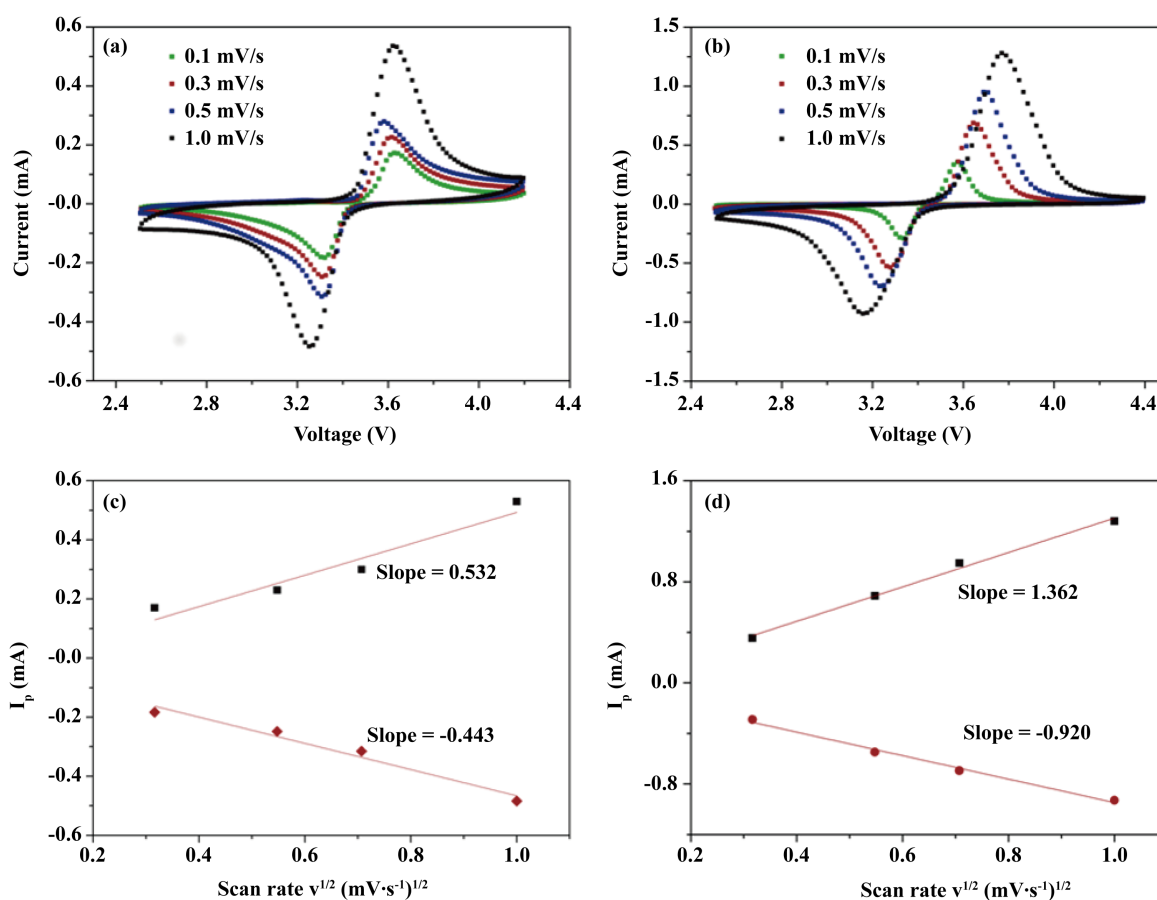


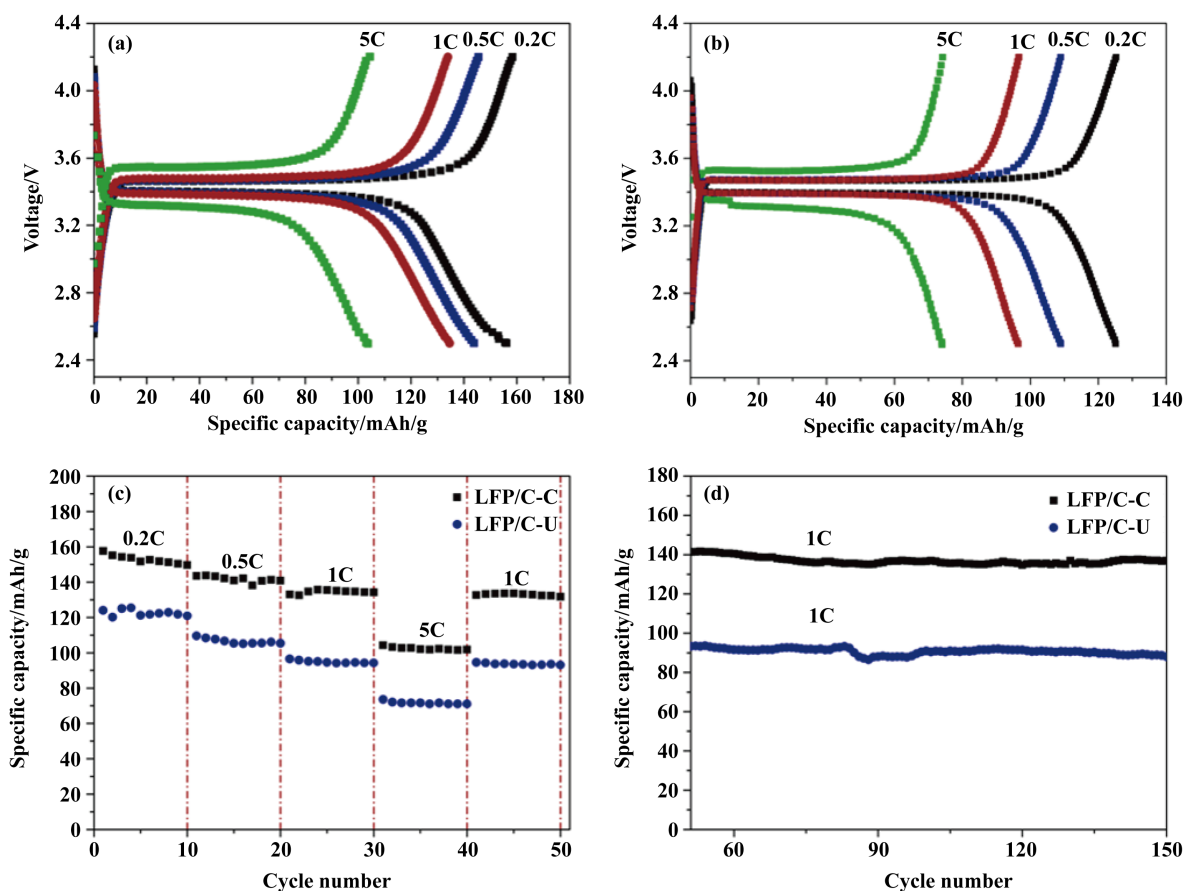
**Figure 4.** CV curves of LFP/C-U (a) and LFP/C-C (b) measured at various scanning rates from  $0.1 \text{ mV}\cdot\text{s}^{-1}$  to  $1.0 \text{ mV}\cdot\text{s}^{-1}$ . The relationship between  $I_p$  and  $v^{1/2}$  determined by CV curves of LFP/C-U (c) and LFP/C-C (d).

liquid electrolyte into the nanofibers and shortens the electrical conducting path. Hence, the enhancement of  $\text{Li}^+$  diffusion coefficient of LFP/C-C can be attributed to its porous structure.

In order to study the electrochemical behavior of the active materials further, galvanostatic charge-discharge performances of LFP/C-C and LFP/C-U were measured at different C-rates (Figure 5(a) and Figure 5(b)). The specific discharge capacities of LFP/C-C at different rates are  $157.7 \text{ mAhg}^{-1}$  (0.2 C),  $143.8 \text{ mAhg}^{-1}$  (0.5 C),  $135.7 \text{ mAhg}^{-1}$  (1 C) and  $104.3 \text{ mAhg}^{-1}$  (5 C), respectively, which are significantly higher than those of LFP/C-U,

**Table 1.** Lithium ion diffusion coefficients of different samples.

Sample		Slope	$D/\text{cm}^2\cdot\text{s}^{-1}$
LFP/C-U	Oxidation peak	0.532	$1.22 \times 10^{-8}$
LFP/C-C	Reduction peak	-0.443	$8.47 \times 10^{-9}$
	Oxidation peak	1.362	$8.00 \times 10^{-8}$
	Reduction peak	-0.920	$3.65 \times 10^{-8}$

**Figure 5.** Charge/discharge curves of LFP/C-C (a) and LFP/C-U (b) electrodes at various rates; discharge capacities at various rates (c) and cycling performances at 1C (d) of LFP/C-C and LFP/C-U electrodes.

*i.e.*  $125.4 \text{ mAhg}^{-1}$  (0.2 C),  $109.6 \text{ mAhg}^{-1}$  (0.5 C),  $96.4 \text{ mAhg}^{-1}$  (1 C) and  $73.5 \text{ mAhg}^{-1}$  (5 C), respectively. Moreover, it is worth noting that the coulombic efficiencies of both LFP/C-C and LFP/C-U are quite high (Figure 5(a) and Figure 5(b)). Comparing the rate performance and cycling performance of LFP/C-C to those of LFP/C-U, plotted in Figure 5(c) and Figure 5(d), it can be concluded that the superior electrochemical performance of LFP/C-C is due to its porous structure.

The EIS spectra of the LFP/C-C and LFP/C-U electrode materials are plotted in Figure 6. The impedance spectra can be understood by an equivalent circuit (the inset of Figure 6), in which  $R_u$  is the uncompensated resistance,  $R_{ct}$  is the charge transfer resistance,  $C_d$  is the double-layer capacitance, and  $Z_w$  is the Warburg impedance.  $R_u$  includes the particle contact resistance, electrolyte resistance, and the resistance between the electrode and the current collector.  $R_{ct}$  is related to the electrochemical reaction at the interface between electrode and electrolyte, and to the contact between the particles. The value of  $R_u$  can be obtained from high frequency intercept of the semicircle, while  $R_{ct}$  is determined by the diameter of the semicircle. The main fitting parameters of

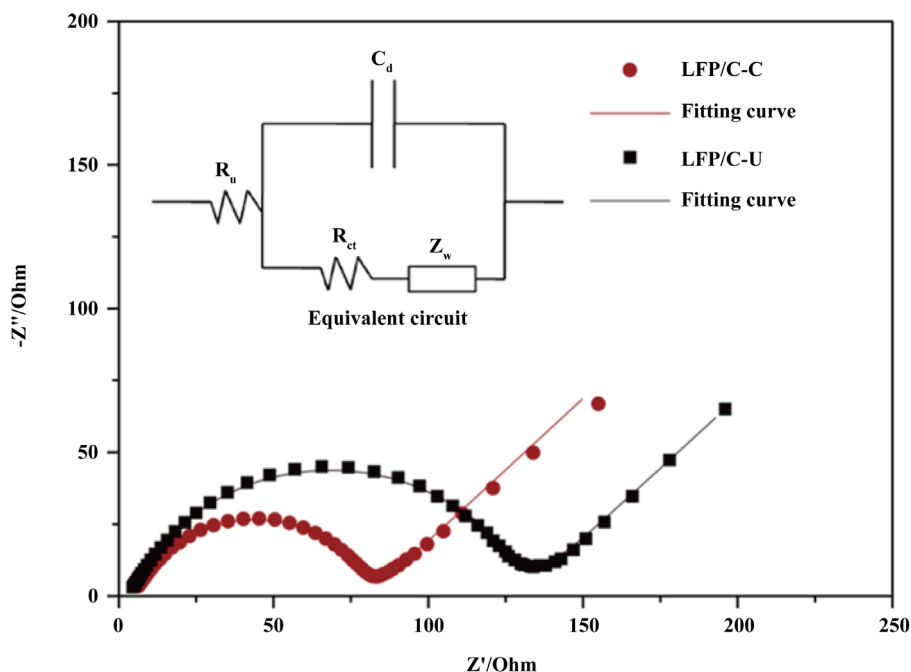


**Figure 6.** Impedance spectra of LFP/C-C and LFP/C-U electrodes recorded in the frequency range from 100 kHz to 10 mHz. The inset is an equivalent circuit of fitting curves.

**Table 2.** Fitting parameters of  $R_u$  and  $R_{ct}$ .

Samples	$R_u/\Omega$	$R_{ct}/\Omega$
LFP/C-C	5.22	76.29
LFP/C-U	3.53	127.7

the equivalent circuit ( $R_u$  and  $R_{ct}$ ) are listed in **Table 2**. It can be seen that the charge transfer resistance of LFP/C-C is clearly lower than that of LFP/C-U, due to the former's porous structure. On the other hand, the total resistance of the equivalent circuit is mainly determined by the sum of  $R_{ct}$  and  $R_u$ . Hence the conductive behavior of LFP/C-C is better than that of LFP/C-U, although the former's  $R_u$  is relatively high. This conclusion is consistent with the results of the conductivity measurements, as discussed above.

#### 4. Conclusion

In summary, nanofibers of LFP/C-C and LFP/C-U cathode materials have been synthesized via a coaxial/uniaxial electrospinning technique followed by sintering. LFP/C-C shows a porous nanofiber morphology, and a layer of amorphous carbon is coated on the surface of the fibers. The electrochemical properties of LFP/C-C, including specific capacity, diffusion coefficient of lithium ion, and overpotential are significantly improved. The enhancement of electrical conductivity and polarization of LFP/C-C is mainly due to the porous morphology and amorphous carbon coating layer, which are strongly related to improved electrochemical performance.

#### Acknowledgements

This work was supported by the National Natural Science Foundation of China (No.61306103), Priority Academic Program Development of Jiangsu Higher Education Institution (PAPD), and the Open Research Fund of Jiangsu Provincial Key Laboratory for Nanotechnology, Nanjing University

#### References

- [1] Liu, H., Yang, H. and Li, J. (2010) A Novel Method for Preparing  $\text{LiFePO}_4$  Nanorods as a Cathode Material for Li-

- thium-Ion Power Batteries. *Electrochimica Acta*, **55**, 1626-1629. <http://dx.doi.org/10.1016/j.electacta.2009.10.039>
- [2] Padhi, A.K., Nanjundaswamy, K.S. and Goodenough, J.B. (1997) Phospho-Olivines as Positive-Electrode Materials for Rechargeable Lithium Batteries. *Journal of The Electrochemical Society*, **144**, 1188-1194. <http://dx.doi.org/10.1149/1.1837571>
- [3] Zhang, W.J. (2011) Structure and Performance of LiFePO<sub>4</sub> Cathode Materials: A Review. *Journal of Power Sources*, **196**, 2962-2970. <http://dx.doi.org/10.1016/j.jpowsour.2010.11.113>
- [4] Liu, Z., Tay, S.W., Hong, L. and Lee, J.Y. (2011) Physical and Electrochemical Characterizations of LiFePO<sub>4</sub>-Incorporated Ag Nanoparticles. *Journal of Solid State Electrochemistry*, **15**, 205-209. <http://dx.doi.org/10.1007/s10008-010-1085-x>
- [5] Gaberscek, M., Dominko, R. and Jamnik, J. (2007) Is Small Particle Size More Important than Carbon Coating? An Example Study on LiFePO<sub>4</sub> Cathodes. *Electrochemistry Communications*, **9**, 2778-2783. <http://dx.doi.org/10.1016/j.elecom.2007.09.020>
- [6] Paolo, P., Lisi, M., Zane, D. and Pasquali, M. (2002) Determination of the Chemical Diffusion Coefficient of Lithium in LiFePO<sub>4</sub>. *Solid State Ionics*, **148**, 45-51. [http://dx.doi.org/10.1016/S0167-2738\(02\)00134-0](http://dx.doi.org/10.1016/S0167-2738(02)00134-0)
- [7] Andersson, A.S., Kalska, B., Haggstrom, L. and Thomas, J.O. (2000) Lithium Extraction/Insertion in LiFePO<sub>4</sub>: An X-Ray Diffraction and Mössbauer Spectroscopy Study. *Solid State Ionics*, **130**, 41-52. [http://dx.doi.org/10.1016/S0167-2738\(00\)00311-8](http://dx.doi.org/10.1016/S0167-2738(00)00311-8)
- [8] Swain, P., Viji, M., Mocherla, P.S.V. and Sudakar, C. (2015) Carbon Coating on the Current Collector and LiFePO<sub>4</sub> Nanoparticles—Influence of sp<sup>2</sup> and sp<sup>3</sup>-Like Disordered Carbon on the Electrochemical Properties. *Journal of Power Sources*, **293**, 613-625. <http://dx.doi.org/10.1016/j.jpowsour.2015.05.110>
- [9] Wang, G., Ma, Z., Shao, G., Kong, L. and Gao, W. (2015) Synthesis of LiFePO<sub>4</sub>@carbon Nanotube Core-Shell Nanowires with a High-Energy Efficient Method for Superior Lithium Ion Battery Cathodes. *Journal of Power Sources*, **291**, 209-214. <http://dx.doi.org/10.1016/j.jpowsour.2015.05.027>
- [10] Zhao, N., Li, Y., Zhi, X., Wang, L., Zhao, X., Wang, Y. and Liang, G. (2016) Effect of Ce<sup>3+</sup> Doping on the Properties of LiFePO<sub>4</sub> Cathode Material. *Journal of Rare Earths*, **34**, 174-180. [http://dx.doi.org/10.1016/S1002-0721\(16\)60011-X](http://dx.doi.org/10.1016/S1002-0721(16)60011-X)
- [11] Naik, A., Zhou, J., Gao, C., Liu, G. and Wang, L. (2016) Rapid and Facile Synthesis of Mn Doped Porous LiFePO<sub>4</sub>/C from Iron Carbonyl Complex. *Journal of the Energy Institute*, **89**, 21-29. <http://dx.doi.org/10.1016/j.joei.2015.01.013>
- [12] Li, J., Zhang, L., Qu, Q., Zhang, L. and Zheng, H. (2013) A Monodispersed Nano-Hexahedral LiFePO<sub>4</sub> with Improved Power Capability by Carbon-Coatings. *Journal of Alloys and Compounds*, **579**, 377-383. <http://dx.doi.org/10.1016/j.jallcom.2013.06.097>
- [13] Li, M., Sun, L., Sun, K., Yu, S., Wang, R. and Xie, H. (2012) Synthesis of Nano-LiFePO<sub>4</sub> Particles with Excellent Electrochemical Performance by Electrospinning-Assisted Method. *Journal of Solid State Electrochemistry*, **16**, 3581-3586. <http://dx.doi.org/10.1007/s10008-012-1790-8>
- [14] Delacourt, C., Poizot, P., Levasseur, S. and Masquelier, C. (2012) Size Effects on Carbon-Free LiFePO<sub>4</sub> Powders. *Electrochemical and Solid-State Letters*, **9**, A352-A355. <http://dx.doi.org/10.1149/1.2201987>
- [15] Wang, J.M., Cai, F.P., Yang, G., Wang, B. and Hu, S.Q. (2015) Synthesis of Porous LiFePO<sub>4</sub>/C Composite Materials by CCVD Method. *Rare Metal Materials and Engineering*, **44**, 307-311. [http://dx.doi.org/10.1016/S1875-5372\(15\)30025-4](http://dx.doi.org/10.1016/S1875-5372(15)30025-4)
- [16] Xie, M., Zhang, X., Wang, Y., Deng, S., Wang, H., Liu, J., Yan, H., Laakso, J. and Levänen, E. (2013) A Template-Free Method to Prepare Porous LiFePO<sub>4</sub> via Supercritical Carbon Dioxide. *Electrochimica Acta*, **94**, 16-20. <http://dx.doi.org/10.1016/j.electacta.2013.01.131>
- [17] Yu, W., Wu, L., Zhao, J., Zhang, Y., Li, G. and Gai, H. (2012) Fabrication of Porous Platelike LiFePO<sub>4</sub>/C Cathode Materials via Hydrothermal Process. *Powder Technology*, **230**, 219-224. <http://dx.doi.org/10.1016/j.powtec.2012.07.034>
- [18] Yang, J., Wang, J., Wang, D., Li, X., Geng, D., Liang, G., Gauthier, M., Li, R. and Sun, X. (2012) 3D Porous LiFePO<sub>4</sub>/Graphene Hybrid Cathodes with Enhanced Performance for Li-Ion Batteries. *Journal of Power Sources*, **208**, 340-344. <http://dx.doi.org/10.1016/j.jpowsour.2012.02.032>
- [19] Yu, F., Lim, S.H., Zhen, Y., An, Y. and Lin, J. (2014) Optimized Electrochemical Performance of Three-Dimensional Porous LiFePO<sub>4</sub>/C Microspheres via Microwave Irradiation Assisted Synthesis. *Journal of Power Sources*, **271**, 231-238. <http://dx.doi.org/10.1016/j.jpowsour.2014.08.009>
- [20] Chen, R., Wu, Y. and Kong, X.Y. (2014) Monodisperse Porous LiFePO<sub>4</sub>/C Microspheres Derived by Microwave-Assisted Hydrothermal Process Combined with Carbothermal Reduction for High Power Lithium-Ion Batteries. *Journal of Power Sources*, **258**, 246-252. <http://dx.doi.org/10.1016/j.jpowsour.2014.02.068>
- [21] Chen, M., Wang, X., Shu, H., Yu, R., Yang, X. and Huang, W. (2015) Solvothermal Synthesis of Monodisperse Mi-

- cro-Nanostructure Starfish-Like Porous  $\text{LiFePO}_4$  as Cathode Material for Lithium-Ion Batteries. *Journal of Alloys and Compounds*, **652**, 213-219. <http://dx.doi.org/10.1016/j.jallcom.2015.08.221>
- [22] Guo, J.X., Chen, L., Zhang, X., Chen, H.X. and Tang, L. (2013) Template-Free Solvothermal Synthesis of Monodisperse Porous  $\text{LiFePO}_4$  Microsphere as a High-Power Cathode Material for Lithium-Ion Batteries. *Materials Letters*, **106**, 290-293. <http://dx.doi.org/10.1016/j.matlet.2013.05.044>
- [23] Chen, Z., Zhao, Q., Xu, M., Li, L., Duan, J. and Zhu, H. (2015) Electrochemical Properties of Self-Assembled Porous Micro-Spherical  $\text{LiFePO}_4$ /PAS Composite Prepared by Spray-Drying Method. *Electrochimica Acta*, **186**, 117-124. <http://dx.doi.org/10.1016/j.electacta.2015.10.143>
- [24] Du, J., Bin Kong, L., Liu, H., Liu, J.B., Liu, M.C., Zhang, P., Luo, Y.C. and Kang, L. (2014) Template-Free Synthesis of Porous- $\text{LiFePO}_4$ /C Nanocomposite for High Power Lithium-Ion Batteries. *Electrochimica Acta*, **123**, 1-6. <http://dx.doi.org/10.1016/j.electacta.2013.12.157>
- [25] Zhu, C., Yu, Y., Gu, L., Weichert, K. and Maier, J. (2011) Electrospinning of Highly Electroactive Carbon-Coated Single-Crystalline  $\text{LiFePO}_4$  Nanowires. *Angewandte Chemie International Edition*, **50**, 6278-6282. <http://dx.doi.org/10.1002/anie.201005428>
- [26] Hosono, E., Wang, Y., Kida, N., Enomoto, M., Kojima, N., Okubo, M., et al. (2011) Synthesis of Triaxial  $\text{LiFePO}_4$  Nanowire with a VGCF Core Column and a Carbon Shell through the Electrospinning Method. *ACS Applied Materials and Interfaces*, **2**, 212-218. <http://dx.doi.org/10.1021/am900656y>
- [27] Qiu, Y., Geng, Y., Li, N., Liu, X. and Zuo, X. (2014) Nonstoichiometric  $\text{LiFePO}_4$ /C Nanofibers by Electrospinning as Cathode Materials for Lithium-Ion Battery. *Materials Chemistry and Physics*, **144**, 226-229. <http://dx.doi.org/10.1016/j.matchemphys.2013.12.027>
- [28] Li, M., Sun, L., Sun, K., Yu, S., Wang, R. and Xie, H. (2012) Synthesis of Nano- $\text{LiFePO}_4$  Particles with Excellent Electrochemical Performance by Electrospinning-Assisted Method. *Journal of Solid State Electrochemistry*, **16**, 3581-3586. <http://dx.doi.org/10.1007/s10008-012-1790-8>
- [29] Kim, J.-K., Cheruvally, G. and Ahn, J.-H. (2008) Electrochemical Properties of  $\text{LiFePO}_4$ /C Synthesized by Mechanical Activation Using Sucrose as Carbon Source. *Journal of Solid State Electrochemistry*, **12**, 799-805. <http://dx.doi.org/10.1007/s10008-007-0425-y>
- [30] Lalia, B.S., Shah, T. and Hashaikeh, R. (2015) Microbundles of Carbon Nanostructures as Binder Free Highly Conductive Matrix for  $\text{LiFePO}_4$  Battery Cathode. *Journal of Power Sources*, **278**, 314-319. <http://dx.doi.org/10.1016/j.jpowsour.2014.12.079>
- [31] Zheng, F., Yang, C., Ji, X., Hu, D., Chen, Y. and Liu, M. (2015) Surfactants Assisted Synthesis and Electrochemical Properties of Nano- $\text{LiFePO}_4$ /C Cathode Materials for Low Temperature Applications. *Journal of Power Sources*, **288**, 337-344. <http://dx.doi.org/10.1016/j.jpowsour.2015.04.126>